# Power Control With Z-Source Converter Based Unified Power Flow Controller

R. Thirumalaivasan, *Member, IEEE*, Yunjian Xu, *Member, IEEE*, and M. Janaki, *Member, IEEE*

***Abstract*—In this paper, we propose a Z-source converter (ZSC)-based unified power flow controller (ZSC-UPFC) to enhance power control for long transmission lines. As a multifunctional controller, the UPFC has been adopted to regulate both the active and reactive power flows in transmission lines and to control the AC bus voltage. A recently proposed converter topology, ZSC, uses a Z-network on its DC side to support the desired AC output voltage. The proposed ZSC-UPFC configuration places a Z-network between the dc-link capacitor and the series converter to boost the series converter DC voltage. The integration of Z-network provides the desired converter voltage even with reduced dc-link capacitor voltage setting. We develop a detailed three-phase model for the proposed ZSC-UPFC by modeling the converter operation with switching functions, which are generated by the space vector pulse width modulation (SVPWM) technique. We conduct linear analysis on the D-Q model as well as extensive transient simulation (based on a detailed nonlinear three-phase model) to evaluate the performance of the overall system with the proposed ZSC-UPFC configuration. Our simulation results demonstrate the effectiveness of ZSC-UPFC: 1) The series converter provides the series compensation in a long transmission line with Z-network, and 2) the shunt converter maintains a constant dc-link capacitor voltage and provides reactive power support for the AC bus.**

***Index Terms*—Power control, space vector pulse width modulation (SVPWM), transient simulation, unified power flow converter (UPFC), Z-source converter (ZSC).**

## I. Introduction

THE introduction of flexible AC transmission systems (FACTS) controllers into power transmission systems provides exciting opportunities to increase the utilization of electrical networks with the existing facilities [1]–[9]. A long transmission line needs controllable series as well as shunt compensation for power flow control and voltage regulation [6]. The unified power flow controller (UPFC) is a flexible and multifunctional FACTS controller. Consisting of a shunt and a series converter, the UPFC can control both the active and reactive power flows in a long transmission line [10], [11]. The shunt converter of a UPFC maintains a constant dc-link voltage and provides reactive power support at the AC bus. The series converter controls the power flow in a long transmission line. The interaction between the series-injected voltage and the transmission line current enables the series converter to exchange active and reactive power with the transmission line.

The active voltage injection of a series converter provides reactive power compensation in the transmission line. In general, the active voltage injection (i.e., resistance emulation) of the series converter supplies/demands active power to/from the dc-link capacitor. As such, the above-mentioned operating mode of the series converter could potentially vary the dc-link capacitor voltage. However, for the proper operation of UPFC, the dc-link capacitor voltage must remain constant. For the conventional voltage-source converter (VSC)-based UPFC, in case the active power demand of the series converter is not met, the dc-link capacitor voltage could collapse and subsequently the UPFC can get disconnected [12]. The shunt converter is designed to supply the active power needed by the series converter via the dc-link capacitor. The shunt converter absorbs/supplies active power from/to the AC bus (of the long transmission line) to maintain the dc-link capacitor voltage at the specified value [7], [10]. As such, the rating of the shunt converter and the dc-link capacitor must be highly rated to support the series converter [10].

A substantial literature is devoted to the application of ZSC in the grid-connected distribution generation systems based on renewable energy sources such as photovoltaic systems, wind turbines, and fuel cell stacks [13]–[15], where the nominal line-to-line voltage is higher than the dc-link voltage. In [16], ZSC is proposed for voltage sag compensation to ensure a constant dc-voltage across the DC link despite the dwindling voltage in storage devices connected to the DC link.

There is growing literature on the application of UPFC in long transmission systems for power flow control and control system design. By varying the magnitude of the series-injected voltage that is in quadrature with the transmission line current, the active power flowing through the long transmission system can be controlled by UPFC [9], [10], [17]. The reactive power flow can be controlled by adjusting the phase angle of the series-injected voltage. This has been achieved by introducing a component of the series-injected voltage to be in-phase with the transmission line current [18]. With UPFC, the D-Q-axis current in a transmission line can be individually controlled to have independent control on both active and reactive power flows in the long transmission line [19], [20]. Wang and Peng [21]

Manuscript received September 1, 2016; revised December 7, 2016; accepted January 22, 2017. Date of publication January 25, 2017; date of current version August 2, 2017. Recommended for publication by Associate Editor D. Vinnikov. *(Corresponding author: Yunjian Xu.)*

R. Thirumalaivasan is with the School of Electrical Engineering, VIT University, Vellore, India, and also with the Engineering Systems and Design Pillar, Singapore University of Technology and Design 487372, Singapore (e-mail: thirumalai22@gmail.com).

Y. Xu is with the Department of Mechanical and Automation Engineering, Chinese University of Hong Kong, Hong Kong (e-mail: xuyunjian@gmail.com).

M. Janaki is with the School of Electrical Engineering, VIT University, Vellore 632014, India (e-mail: janaki.m@vit.ac.in).

Digital Object Identifier 10.1109/TPEL.2017.2657798

propose a new configuration of UPFC, where cascade multilevel inverters are used to lower the cost, volume, and increase the system reliability.

Closely related to this work, Sadigh *et al.* [22] seek to minimize the power rating of the shunt converter in UPFC for active and reactive power by adding series capacitor in the transmission line. However, the presence of series capacitor in the transmission line will prone to subsynchronous resonance [23], [24]. In this work, we aim to reduce the power rating of the UPFC shunt converter by introducing Z-network in the series converter to boost the DC voltage of the series converter.

The high rating of the shunt converter and the dc-link capacitor in conventional UPFC design motivates us to incorporate Z-network into an UPFC to boost the DC voltage across the series converter without highly rated dc-link capacitor. In power conversion, the impedance-source converter (ZSC) has the capability to either buck or boost voltage [25]. The ZSC permits the shoot-through between upper and lower power switches on any phase leg, and therefore achieves voltage boost capability by inserting shoot-through states in the converter PWM switching pattern [26]–[30]. By controlling the shoot-through duty cycle, ZSC can provide any desired AC output voltage. The main advantages of ZSC are insensitivity to DC bus voltage variation and increased reliability.

In this paper, we propose a ZSC-based UPFC (ZSC-UPFC) to enhance the power control in a long transmission line. To our knowledge, this work is *the first* that proposes and analyzes ZSC-UPFC for power transmission systems. In order to support the series converter compensation, the Z-network is placed between the dc-link capacitor and the series converter (see Fig. 1). When the demand on the series converter voltage increases, it can be met by the ZSC boost factor $(B > 1)$ without increasing the dc-link voltage. The proposed ZSC-UPFC supports the active power demand of the series converter with the steady DC boosted voltage. As a result, the proposed ZSC-UPFC can function more effectively than the conventional VSC-based UPFC under transient states of a long transmission line. In general, the shoot-through ratio controller helps to reduce the rating of the shunt converter and the dc-link capacitor. Furthermore, the shoot-through ratio controller also enables the shunt converter to absorb less active power from the AC bus. In the proposed ZSC-UPFC, when the reference setting of the dc-link voltage controller reduces, the boost factor is regulated to rise in order to maintain the series-injected voltage at a constant value. Compared to the conventional UPFC, the proposed ZSC-UPFC can significantly reduce the voltage rating of the shunt converter and the dc-link capacitor.

Our analysis is based on a detailed three-phase model of two-level ZSC-UPFC, in which the converter operation is modeled by switching functions. In our analysis, the space vector pulse width modulation (SVPWM) technique is used to generate the switching function of both converters. In this paper, we adopt the implementation of the SVPWM technique for a two-level converter originally proposed in [31]–[33].

The performance of combined system with the proposed ZSC-UPFC configuration and its control method are validated by transient simulation. Simulation results demonstrate the effectiveness of the proposed ZSC-UPFC to provide series compensation in the long transmission line with shoot-through state. Simulation results also show that the shunt converter maintains a constant dc-link voltage and provides reactive power control at AC bus. The incorporation of ZSC in UPFC helps to reduce the power rating of the shunt converter and the dc-link capacitor (see Section III-E).

The paper is organized as follows. In Section II, we present the modeling of ZSC-UPFC. In Section III, we present the control method and space vector modulation of ZSC-UPFC. In Section IV, we validate the performance of the proposed ZSC-UPFC through transient analysis and simulation. Some brief concluding remarks are given in Section V.

## II. Proposed System: ZSC-UPFC

The schematic representation of ZSC-UPFC as a part of the IEEE first bench mark (FBM) [34] is shown in Fig. 1. The IEEE FBM model is adapted in our study: The overall system consists of a turbine, a generator (2.2 model in [34]), as well as a shunt VSC and a series ZSC connected to *a long transmission line*. ZSC injects a series voltage while the shunt VSC is controlled to inject the reactive current. The parameters (all in p.u.) of the overall system are given in the Appendix.

The dc- and ac-side modeling of the proposed ZSC-UPFC will be introduced in the following two sections.

### A. DC-Side Modeling of ZSC-UPFC

The equivalent circuit of shoot-through and nonshoot-through states of ZSC are represented in Fig. 2(a) and (b), respectively [27]. In the shoot-through state, the Z-network capacitors transfer their stored energy to inductors. Whereas in the nonshoot-through state, the DC power source charges the Z-source capacitors and delivers power to the system. In the nonshoot-through state, the Z-source inductors also release their stored energy to the system, which in turn boosts the DC voltage across the series converter.

The peak DC voltage $\widehat{V}_{\rm dcz}$ and the peak AC output voltage $\widehat{V}^i_{\rm se}$ of the series converter are expressed as

$$\widehat{V}_{\rm dcz} = 2V_c - V_{\rm dc} = \frac{1}{1-\frac{2T_{\rm sh}}{T}} V_{\rm dc} = BV_{\rm dc}, \tag{1}$$

$$\widehat{V}^i_{\rm se} = M_{\rm se} V_{\rm dcz} = M_{\rm se} B V_{\rm dc}, \quad 0 \le \frac{T_{\rm sh}}{T} < 0.5 \tag{2}$$

where the superscript $i$ in $V^i_{\rm se}$ and $V^i_{\rm sh}$ represents converter output values. $T_{\rm sh}$ and $T$ denote the shoot-through interval and the switching period, respectively, and $B(>1)$ is the boost factor introduced by the shoot-through state. $M_{\rm se}$ is the modulation index (that is commonly used for conventional converters), where the subscript $se$ represents the series converter. We consider a symmetric ZSC with inductor currents $I_{L1} = I_{L2} = I_L$ and capacitor voltages $V_{c1} = V_{c2} = V_c$. From (2), we note that the

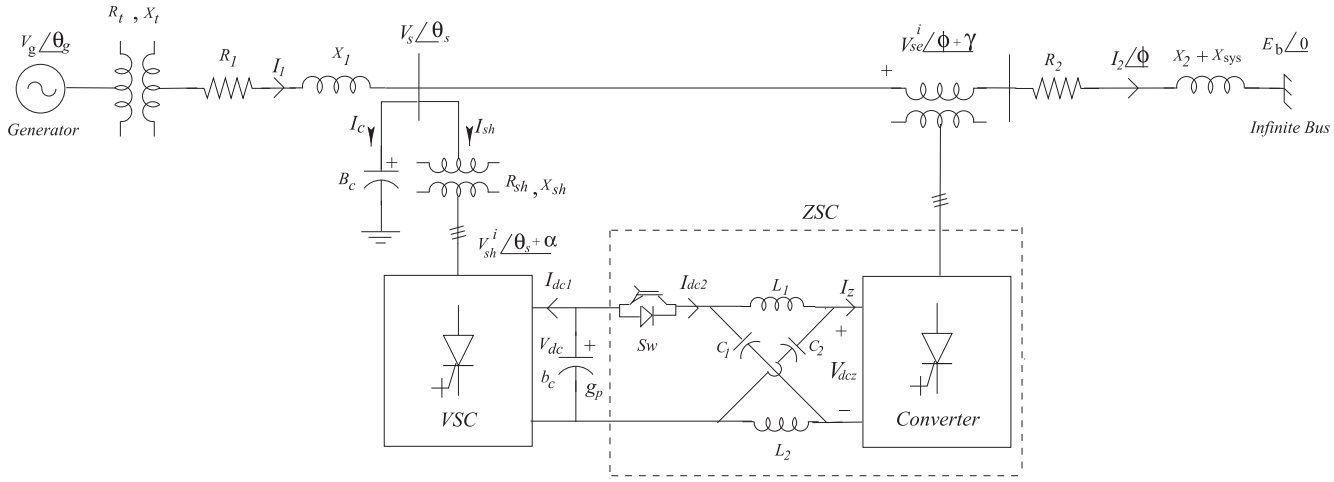


Fig. 1. Modified IEEE first bench mark model with Z-source converter-based UPFC.

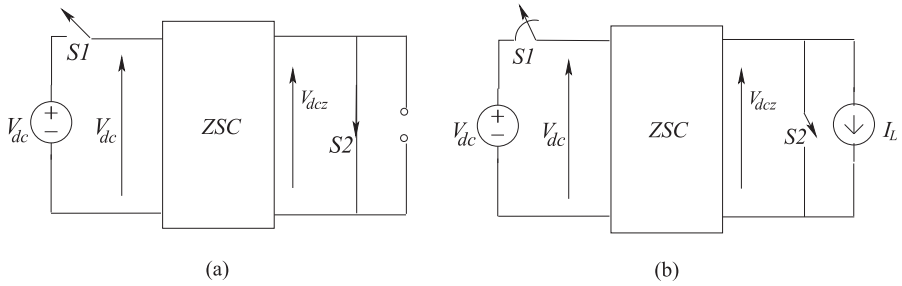


Fig. 2. Equivalent circuit representation of ZSC in (a) the shoot-through state and (b) the nonshoot-through state.

peak AC output voltage of ZSC can either be bucked by reducing $M_{\rm se}$ and maintaining $B = 1$, or boosted by increasing $B$ above unity in the steady state.

As in [27], we can write the dynamic state average equations of ZSC with both shoot-through and nonshoot-through states as

$$\frac{dI_{L1}}{dt} = -\frac{(r+R)}{L}I_{L1} + \frac{D_S}{L}V_{c1} - \frac{D_A}{L}V_{c2} + \frac{D_A}{L}(V_{\rm dcz} + RI_z), \quad (3)$$

$$\frac{dI_{L2}}{dt} = -\frac{(r+R)}{L}I_{L2} - \frac{D_A}{L}V_{c1} + \frac{D_S}{L}V_{c2} + \frac{D_A}{L}(V_{\rm dcz} + RI_z), \quad (4)$$

$$C\frac{dV_{c1}}{dt} = -D_S I_{L1} + D_A I_{L2} - D_A I_z, \quad (5)$$

$$C\frac{dV_{c2}}{dt} = D_A I_{L1} - D_S I_{L2} - D_A I_z \quad (6)$$

where $D_S$ is the shoot-through duty ratio, and $D_A$ is the nonshoot-through duty ratio, $R$ is the equivalent series resistance of the Z-network capacitor, and $r$ is the parasitic resistance of the Z-network inductor.

The series and shunt branches of the proposed ZSC-UPFC can generate/absorb reactive power independently and exchange active power. As such, a bidirectional switch is put between the Z-network and the dc-link capacitor to enable active power exchange between the shunt and the series converter. We can write the dynamics of dc-link capacitor as

$$C_{\rm dc}\frac{dV_{\rm dc}}{dt} = -g_p V_{\rm dc} - I_{\rm dc1} - D_A I_{\rm dc2} \quad (7)$$

where $C_{\rm dc}$ and $g_p$ are the capacitance and conductance of the dc-link capacitor, respectively.

### *B. AC-Side Modeling of ZSC-UPFC*

The ac-side dynamics of the shunt converter in *D–Q* variables are given by [6]

$$\frac{dI_{\rm shD}}{dt} = -\frac{R_{\rm sh}\omega_b}{X_{\rm sh}}I_{\rm shD} - \omega_o I_{\rm shQ} + \frac{\omega_b}{X_{\rm sh}}(V_{sD} - V^i_{\rm shD}), \quad (8)$$

$$\frac{dI_{\rm shQ}}{dt} = -\frac{R_{\rm sh}\omega_b}{X_{\rm sh}}I_{\rm shQ} + \omega_o I_{\rm shD} + \frac{\omega_b}{X_{\rm sh}}(V_{sQ} - V^i_{\rm shQ}) \quad (9)$$

where $\omega_b$ is the base frequency, $R_{\rm sh}$ is the shunt transformer resistance, and $X_{\rm sh}$ is the shunt transformer reactance. The shunt converter output voltage $V^i_{\rm sh}$ can be represented in the D-Q frame as [7]

$$V^i_{\rm sh} = \sqrt{{V^i_{\rm sh_D}}^2 + {V^i_{\rm sh_Q}}^2}, \quad (10)$$

$$V^i_{\rm sh_D} = M_{\rm sh}V_{\rm dc}\sin(\theta_s + \alpha), \quad (11)$$

$$V^i_{\mathrm{sh_Q}} = M_{\mathrm{sh}} V_{\mathrm{dc}} \cos(\theta_s + \alpha). \quad (12)$$

Similarly, the series converter output voltage can be represented in the D-Q frame as [7]

$$V^i_{\mathrm{se}} = \sqrt{{V^i_{\mathrm{seD}}}^2 + {V^i_{\mathrm{seQ}}}^2}, \quad (13)$$

$$V^i_{\mathrm{seD}} = M_{\mathrm{se}} B V_{\mathrm{dc}} \sin(\phi + \gamma), \quad (14)$$

$$V^i_{\mathrm{seQ}} = M_{\mathrm{se}} B V_{\mathrm{dc}} \cos(\phi + \gamma). \quad (15)$$

## III. ZSC-UPFC Controller and SVPWM

In the proposed ZSC-UPFC, the dc-link capacitor voltage is regulated at the specified value by the DC voltage controller to maintain power balance between its shunt and series branches. As mentioned earlier, the series and shunt branches can exchange active power, and generate/absorb reactive power independently. The shoot-through duty ratio controller of ZSC is designed to maintain the series converter DC voltage at the specified value.

The designed shunt converter controller and the series converter controller are illustrated in Figs. 3 and 4, respectively. The output of these two controllers are provided to SVPWM so as to generate the switching functions of the corresponding converters. In the following five sections we introduce the control methods and SVPWM modulation process.

### A. Shunt Converter Controller

The active/reactive currents of the shunt converter are controlled by varying the active/reactive modulation indices [35]. The DC voltage controller of the shunt converter is designed to maintain a constant dc-link capacitor voltage. The shunt converter controller is properly designed to guarantee a constant dc-link capacitor voltage by absorbing/supplying active power from/to the power system when there is decrease/increase in dc-link capacitor voltage. The reference value of the reactive current can be either held constant or regulated to control the reactive power and/or bus voltage magnitude.

In Fig. 3, active and reactive currents are given by

$$I_{\mathrm{Psh}} = I_{\mathrm{shD}} \sin\theta_s + I_{\mathrm{shQ}} \cos\theta_s, \quad (16)$$

$$I_{\mathrm{Rsh}} = -I_{\mathrm{shD}} \cos\theta_s + I_{\mathrm{shQ}} \sin\theta_s. \quad (17)$$

Based on the outputs of the shunt converter controller, $V^i_{\mathrm{shD}}$ and $V^i_{\mathrm{shQ}}$ are calculated according to (11) and (12) as shown in the calculation block. We then obtain the reference value of $V^i_{\mathrm{sh(abc)}}$ using the D-Q to three-phase transformation.

### B. Series Converter Controller

In ZSC, the active/reactive modulation indices are modulated to control active/reactive power in transmission line. The active/reactive modulation indices are regulated through the modulation index $M_{\mathrm{se}}$ or the boost factor $B$ [14], [27].

The structure of controller for the series converter is shown in Fig. 4. The injected active and reactive voltages in terms of variables in the D-Q frame ($V^i_{\mathrm{seD}}$ and $V^i_{\mathrm{seQ}}$) are given by

$$V_{\mathrm{Pse}} = V^i_{\mathrm{seD}} \sin\phi + V^i_{\mathrm{seQ}} \cos\phi, \quad (18)$$

$$V_{\mathrm{Rse}} = V^i_{\mathrm{seD}} \cos\phi - V^i_{\mathrm{seQ}} \sin\phi. \quad (19)$$

Here, a positive $V_{\mathrm{Rse}}$ implies that the VSC injects inductive voltage and a positive $V_{\mathrm{Pse}}$ implies that the VSC draws active power from the transmission line. In the series controller, the reference active/reactive modulation indices are derived from the constant resistance emulation $R_{\mathrm{se}}$ controller and the constant reactance emulation $X_{\mathrm{se}}$ controller, respectively.

Based on the outputs of the series converter controller, $V^i_{\mathrm{seD}}$ and $V^i_{\mathrm{seQ}}$ are calculated according to (14) and (15) as shown in the calculation block. We then obtain the reference value of $V^i_{\mathrm{se(abc)}}$ using the D-Q to three-phase transformation.

Under the inductive mode of the series converter, i.e., with the positive reactance emulation, its AC output voltage is regulated by varying either the modulation index $M_{\mathrm{se}}$ or the boost factor $B$ above unity in the steady state. With the negative reactance emulation (under the capacitive mode), by maintaining $B$ at unity, the modulation index $M_{\mathrm{se}}$ is varied to control the AC output voltage.

### C. Shoot-Through Duty Ratio Controller

We employ the two loop control strategy (originally proposed in [14]) to control the shoot-through duty ratio of Z-source series control. The structure of the shoot-through duty ratio controller is shown in Fig. 5. According to this control strategy, the reference value of the inductor current is controlled to maintain the series converter DC voltage setting. The inner current loop is closed by cascading a proportional controller for faster response. The low-pass filter at the output of controller structure incurs a measurement delay. A measurement delay of 2 ms is adopted in our model. The feedback signal is derived using the measured capacitor voltage and shoot-through duty ratio. The shoot-through duty ratio controller is designed to maintain the series converter DC voltage at the specified value.

The reference voltage of the shunt/series converter is determined by the output of the shunt/series controller, respectively. Subsequently, the switching functions of these two converters are generated using the reference voltages. We apply the SVPWM technique to generate the switching functions of converters. In the following section, we present the SVPWM process.

### D. SVPWM for ZSC-UPFC

The objective of the SVPWM technique is to approximate the desired output voltage by setting proper switching patterns of the converter switches. In SVPWM, the reference voltage vector $\overrightarrow{V}_{\mathrm{ref}}$ of the three-phase converter is obtained by mapping the desired three-phase voltages to the two-dimensional plane as follows:

$$\overrightarrow{V}_{\mathrm{ref}} = V_{\mathrm{dc}} \begin{bmatrix} \frac{2}{\sqrt{6}} & -\frac{1}{\sqrt{6}} & -\frac{1}{\sqrt{6}} \\ 0 & \frac{1}{\sqrt{2}} & -\frac{1}{\sqrt{2}} \end{bmatrix} \begin{bmatrix} a \\ b \\ c \end{bmatrix} \quad (20)$$

where $[a\ b\ c]^T$ is the switching variable vector. The value of the switching variable is either 0 (for switch OFF) or 1 (for switch

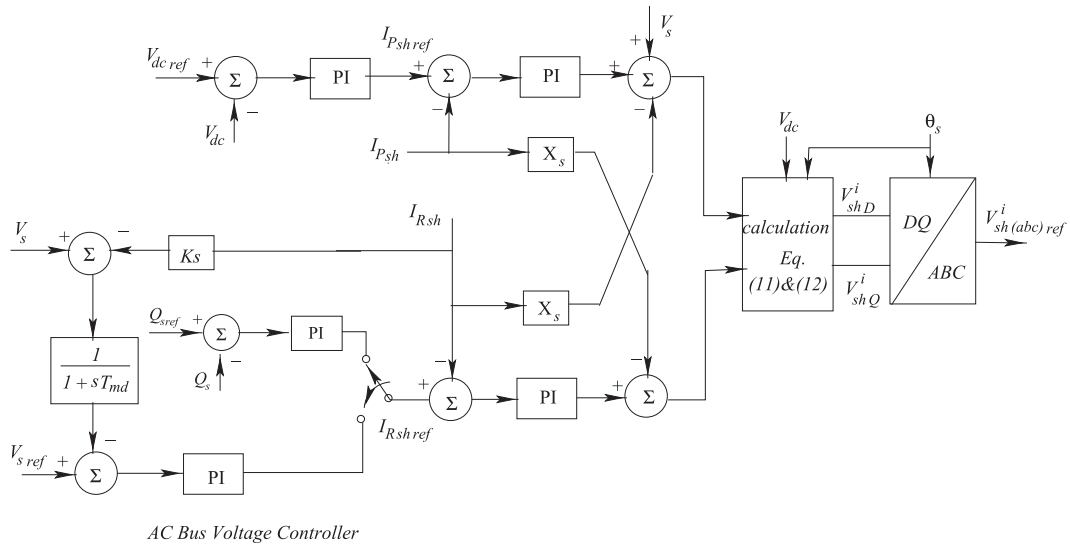


Fig. 3. Shunt converter controller.

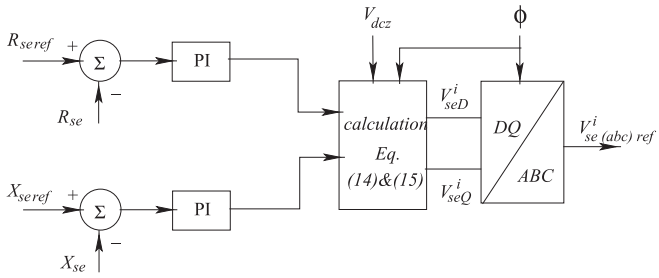


Fig. 4. Series converter controller.

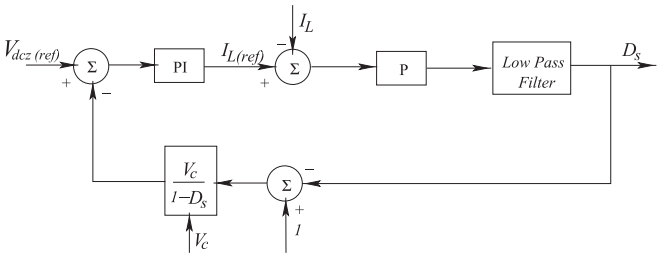


Fig. 5. Shoot-through duty ratio controller.

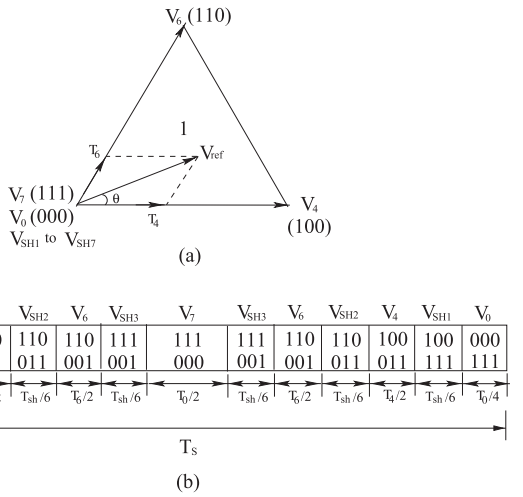


Fig. 6. (a) Space vector diagram in sector 1 $(0 \leq \theta \leq \pi/3)$ for a three-phase ZSC. (b) SVPWM switching sequence in sector 1 for a three-phase ZSC.

ON). Generally, in the space vector modulation, the reference vector $\overrightarrow{V}_{\rm ref}$ is synthesized with three space vectors nearest to the reference vector [33].

The SVPWM implemented based on the two-level converter model (proposed in [32], [33]) will output six active voltage vectors and two null vectors. In conventional SVPWM, the desired output voltage vector $V_{\rm ref}$ is approached by the linear combination of these active and null vectors, whereas along with ZSC the SVPWM uses active, null, and the shoot-through vectors to obtain the desired output voltage vector.

The selection of the active vectors depends on the phase angle $\theta = \omega t$, and this can be easily implemented once the phase angle is detected. With the selected vectors, we compute the time duration of each vector. The switching sequence of ZSC is determined by inserting appropriate shoot-through states in the seven-segment switching sequence of a conventional SVPWM. For instance, Fig. 6(a) and (b) shows the space vector diagram in sector 1 $(0 \leq \theta \leq \pi/3)$ and the SVPWM switching sequence in sector 1 for a three-phase ZSC. Fig. 6(b) depicts the time duration of each vector in one switching time period $(T_s)$ and the symmetric allocation of the shoot-through vectors in the ZSC switching sequence. The switching sequences for other sectors can be calculated in a similar manner. $U$ and $L$ in Fig. 6(b) refer to the upper and lower switch states, respectively. In the SVPWM switching sequence, the appropriate shoot-through states are carefully selected and evenly inserted between each pair of the active and null vectors. As such, the SVPWM technique approximates the desired output voltage by setting proper switching patterns of converter switches.

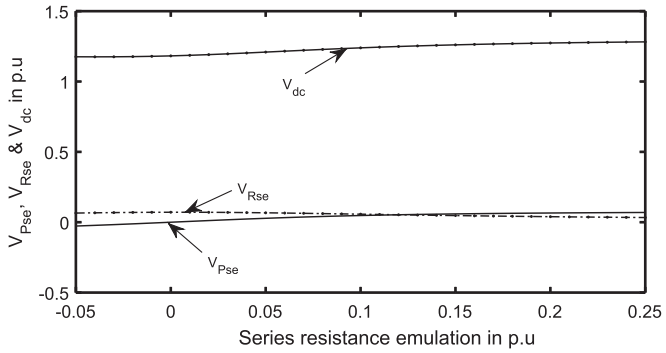


Fig. 7. UPFC without ZSC: The values of dc-link capacitor voltage ($V_{\rm dc}$), series active voltage injection ($V_{\rm Pse}$), and series reactive voltage injection ($V_{\rm Rse}$) under various series resistance emulation.

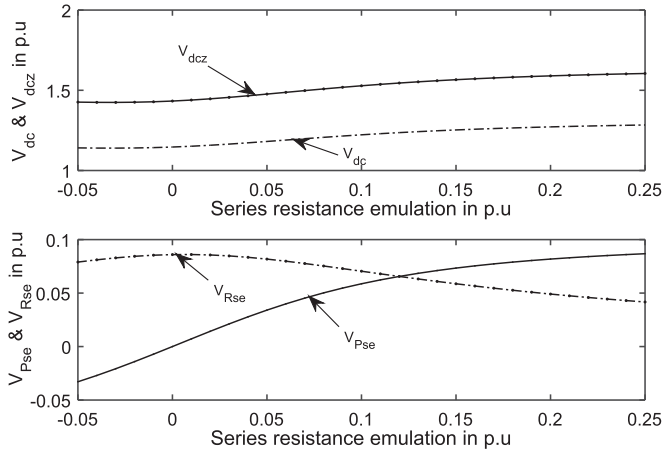


Fig. 8. Proposed ZSC-UPFC: The values of dc-link capacitor voltage ($V_{\rm dc}$), series converter DC voltage ($V_{\rm dcz}$), series active voltage injection ($V_{\rm Pse}$), and series reactive voltage injection ($V_{\rm Rse}$) under various series resistance emulation.

### *E. Comparison With the Conventional UPFC*

In a conventional UPFC, the proper operation of both (the shunt and series) converters depends on the dc-link capacitor voltage. In general, the active voltage injection (i.e., resistance emulation) of a series converter could potentially vary the dc-link capacitor voltage. For a conventional UPFC (without ZSC), Fig. 7 shows the values of the dc-link capacitor voltage, the series active voltage injection, and the series reactive voltage injection, when the shunt converter operates under reactive power control mode and the series converter operates under resistance emulation mode. We observe from Fig. 7 that the required value of dc-link capacitor voltage is increasing with the series resistance emulation. The active voltage injection is also increasing with the series resistance emulation, whereas the reactive voltage injection can decrease with the series resistance emulation. These simulation results indicate that the power rating of the dc-link capacitor and the shunt converter must be increasing, as the need of series active voltage injection increases.

The incorporation of the ZSC into an UPFC helps to boost the DC voltage across the series converter without a highly rated dc-link capacitor. Fig. 8 shows the values of dc-link capacitor voltage, series converter DC voltage, series active voltage injection, and series reactive voltage injection for the proposed ZSC-UPFC with 0.1 shoot-through duty ratio. Interestingly, we observe from Fig. 8 that the DC voltage across the series converter $V_{\rm dcz}$ is increasing with the series resistance emulation. The active voltage injection is also increasing with the series resistance emulation, whereas the reactive voltage injection can decrease with the series resistance emulation after some point. Comparing the almost flat dc-link capacitor voltage ($V_{\rm dc}$) in Fig. 7 and the boosted series converter DC voltage ($V_{\rm dcz}$) in Fig. 8, we conclude that the active power demand of the series converter can be largely met by the ZSC. As a result, the power rating of the dc-link capacitor and the shunt converter can be significantly reduced.

TABLE I
EIGENVALUES OF THE LINEAR SYSTEM

| Eigenvalues | | | |
|---|---|---|---|
| ZSC-UPFC | | Transmission Network | Generator |
| $-437.81 \pm j\ 137.52$ | $-1946.7 \pm j\ 4743.6$ | $-139.12 \pm j\ 2551.7$ | $-0.4598 \pm j\ 6.6724$ |
| $-5.1414 \times 10^5$ | $-6.2832 \pm j\ 4442.9$ | $-110.69 \pm j\ 1904.6$ | $-0.2064 \pm j\ 98.957$ |
| $-4.5661 \times 10^5$ | $-21.322 \pm j\ 6.4831$ | Shunt capacitor | $-0.0726 \pm j\ 127.01$ |
| $-86824, -16845$ | $-6.4452 \times 10^5$ | | $-0.6436 \pm j\ 160.57$ |
| $-73.572, -79.916$ | $-1.5462 \times 10^5$ | $-1.3023 \pm j\ 352.29$ | $-0.3636 \pm j\ 202.93$ |
| $-19.644, -5.033$ | $-31357, -33.01, -20.146$ | | $-1.8504 \pm j\ 298.17$ |

## IV. EIGENVALUE AND TRANSIENT SIMULATION

In MATLAB-Simulink [36], we construct two models for the proposed ZSC-UPFC (shown in Fig. 1): a D-Q model and a nonlinear three-phase model. In the following sections, we will validate the performance of the proposed ZSC-UPFC through eigenvalue analysis (based on the D-Q model) and transient simulation (based on both the D-Q and the three-phase models).

### *A. Eigenvalue Analysis*

Through eigenvalue analysis we seek to validate the stability of the system with the D-Q model of ZSC-UPFC. Table I shows the eigenvalues of the system matrix of the linearized system with $D_S = 0.1$. From Table I, we observe that all the eigenvalues have negative real parts and therefore the system is stable.

The variation of the shoot-through duty ratio could change the series resistance and reactance emulation, and subsequently affect the eigenvalues of the system. It is therefore important to monitor the movement of eigenvalues through the variation of the shoot-through duty ratio. In Fig. 9, we present the eigenvalues of the system (with the shoot-through duty ratio varying from 0 to 0.18) in the complex plane. From Fig. 9, we note that the variation of the shoot-through duty ratio (from 0 to 0.18) has the minimum effect on the eigenvalues. These results demonstrate that the system is stable for all the values of the

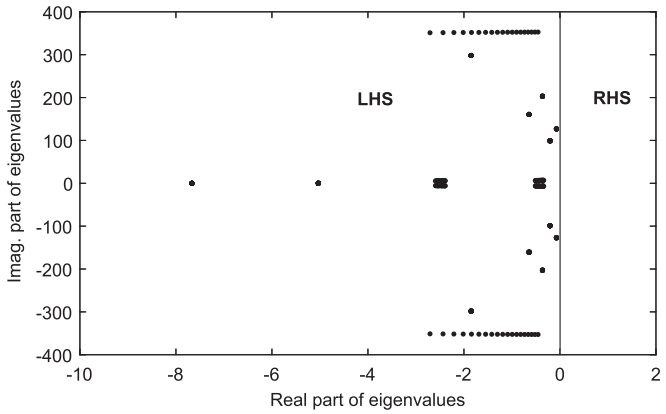


Fig. 9. System eigenvalues shown in the complex plane with varying shoot-through duty ratios (from 0 to 0.18).

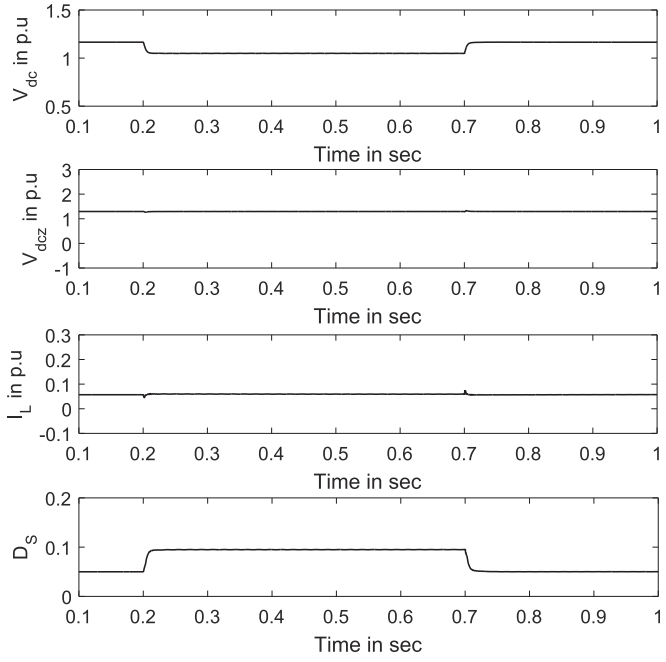


Fig. 10. Step change in the dc-link capacitor voltage $V_{\rm dc}$, and the responses of the series converter DC voltage ($V_{\rm dcz}$), the inductor current ($I_L$), and the shoot-through duty ratio ($D_S$) to the step change in $V_{\rm dc}$, based on the D-Q model of ZSC-UPFC.

shoot-through duty ratio in the set range, and that the eigenvalues are not significantly affected by the shoot-through duty ratio.

### *B. Transient Response of the DC-Link Capacitor Voltage*

To validate the performance of the proposed ZSC-UPFC, we carry out transient simulation on both the D-Q and the three-phase models of the proposed ZSC-UPFC. The step change of $10\%$ decrease in the reference setting of the dc-link capacitor voltage is applied at 0.2 s in our transient simulation. The dc-link capacitor voltage is set back to normal at 0.7 s. We observe from Figs. 10 and 11 that the transient simulation results based on the D-Q and the three-phase models (of the proposed ZSC-UPFC) are consistent. We note from Figs. 10 and 11 that as the

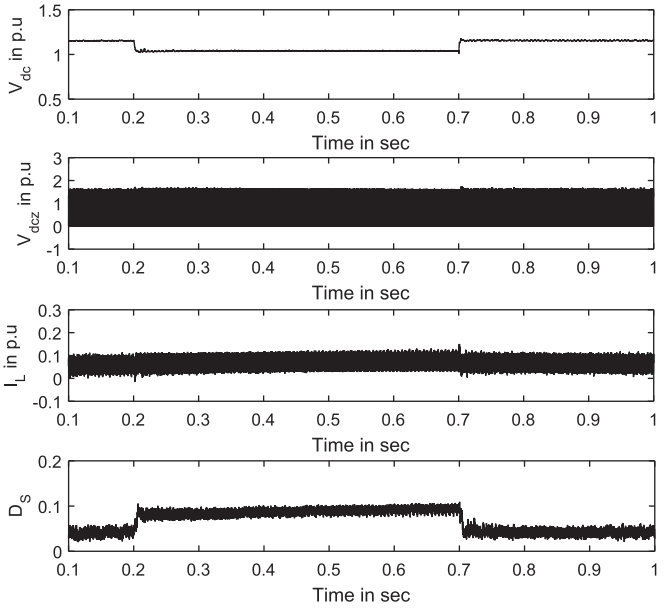


Fig. 11. Step change in the dc-link capacitor voltage $V_{\rm dc}$, and the responses of the series converter DC voltage ($V_{\rm dcz}$), the inductor current ($I_L$), and the shoot-through duty ratio ($D_S$) to the step change in $V_{\rm dc}$, based on the nonlinear three-phase model of ZSC-UPFC.

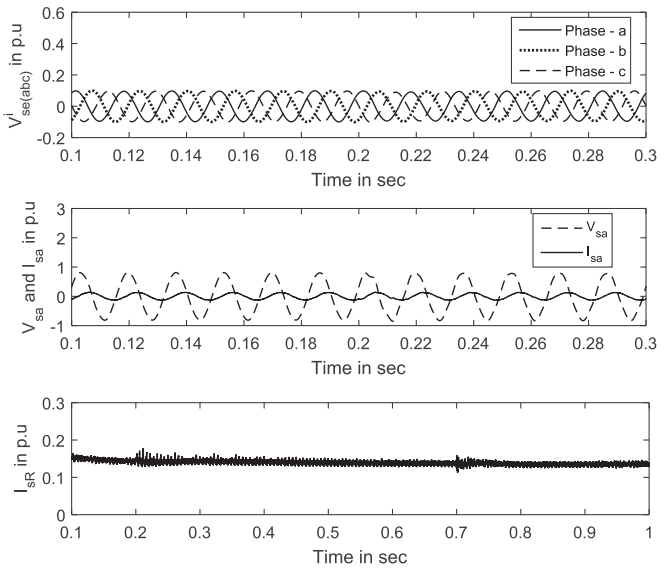


Fig. 12. Response to the step change in dc-link capacitor voltage of series-injected three-phase voltages ($V^i_{\rm se(abc)}$), phase-$a$ of AC bus voltage ($V_{sa}$)/shunt converter current ($I_{sa}$), and shunt converter reactive current ($I_{sR}$).

reference setting of the dc-link capacitor voltage is reduced, the shoot-through duty ratio increases. This is because the shoot-through duty ratio controller operates to maintain the series converter DC voltage $V_{\rm dcz}$ at the specified value. Hence, the series voltage injection is maintained at the specified value. The step responses shown in Figs. 11 and 12 demonstrate the effectiveness of the Z-source-based series converter in providing series compensation even when the reference setting of dc-link capacitor voltage is reduced.

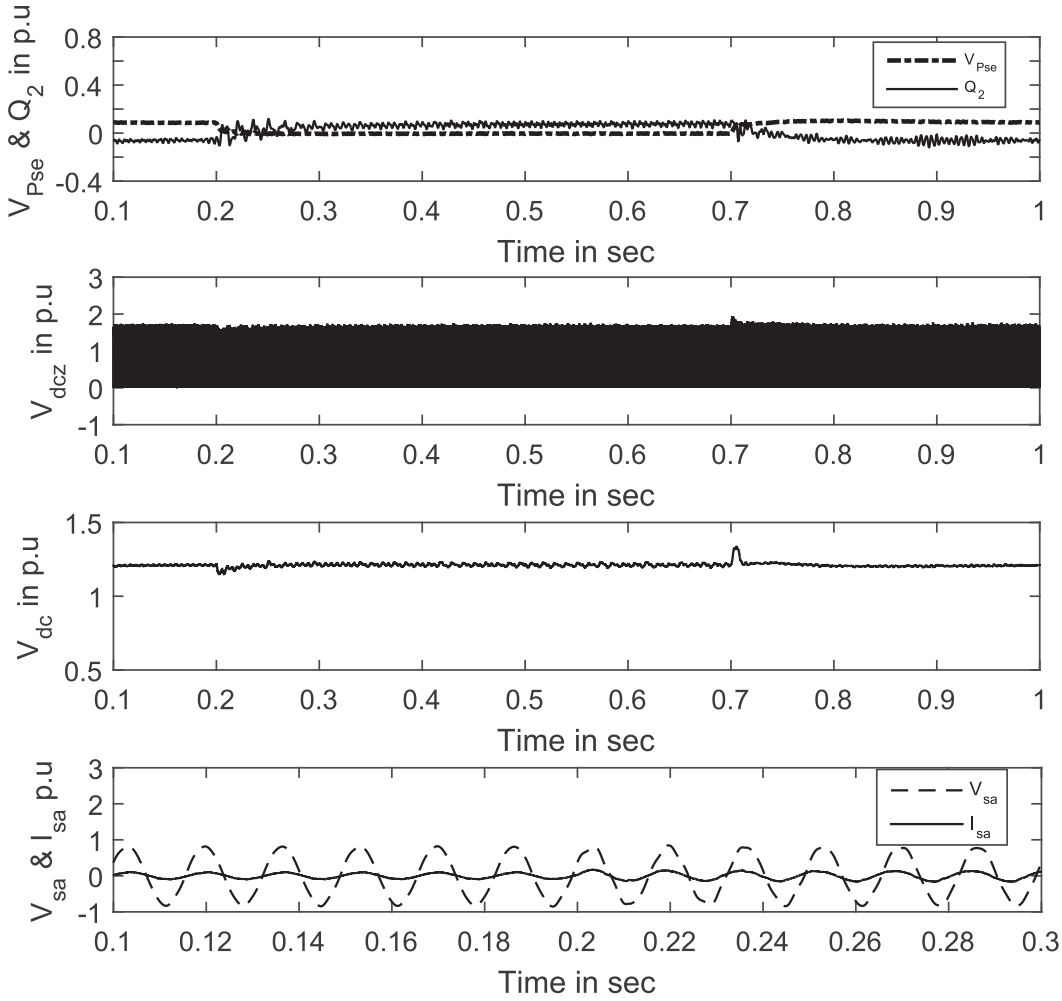


Fig. 13. Response to the step change in resistance emulation of Z-source series converter of the series-injected active voltage ($V_{\mathrm{Pse}}$), reactive power in the line ($Q_2$), series converter DC voltage ($V_{\mathrm{dcz}}$), dc-link capacitor voltage ($V_{\mathrm{dc}}$), and phase-$a$ of AC bus voltage ($V_{sa}$)/shunt converter current ($I_{sa}$).

### C. Active Voltage Injection of the Z-Source Series Converter

The active voltage injection of the series converter provides reactive power compensation through positive/negative resistance emulation. To validate the performance of the proposed ZSC-UPFC, a step change in resistance emulation $R_{\mathrm{se}}$ is applied at 0.2 s, and is removed at 0.7 s. Fig. 13 shows the response of the Z-source series converter to the step change in resistance emulation. We note from Fig. 13 that the series active voltage changes from positive to negative at the step change in resistance emulation. As a result, the reactive power in the transmission line changes from negative to positive. The step responses shown in Fig. 13 demonstrate the effectiveness of the Z-source series converter in providing series reactive power compensation to transmission lines.

### D. Reactive Voltage Injection of the Z-Source Series Converter

The reactive voltage injection of the series converter provides active power compensation through positive/negative reactance emulation. Under the inductive (capacitive) mode, the series converter injects positive (negative, respectively) reactive voltage. To validate the performance of the proposed ZSC-UPFC, a step change in reactance emulation $X_{\mathrm{se}}$ is applied at 0.2 s, and is removed at 0.7 s, leading to a transition from capacitive mode to inductive mode. The boost factor $B$ of a capacitive mode series converter is maintained at unity. We observe from Fig. 14 that the series reactive voltage changes from positive to negative in response to the step change of reactance emulation. As a result, the active power flow in the transmission line increases due to the negative reactive voltage injection of the Z-source series converter. We note from Fig. 15 that when the shoot-through duty ratio goes zero, the value of the series converter DC voltage reaches the dc-link capacitor voltage. The step responses shown in Figs. 14 and 15 demonstrate the effectiveness of Z-source-based series converter in providing series active power compensation through capacitive/inductive mode operation.

### E. Inductive and Capacitive Mode Operation of the Shunt Converter

The shunt converter provides reactive power support at the AC bus where it is connected. To validate the performance of the shunt converter, a step change in the reactive current reference

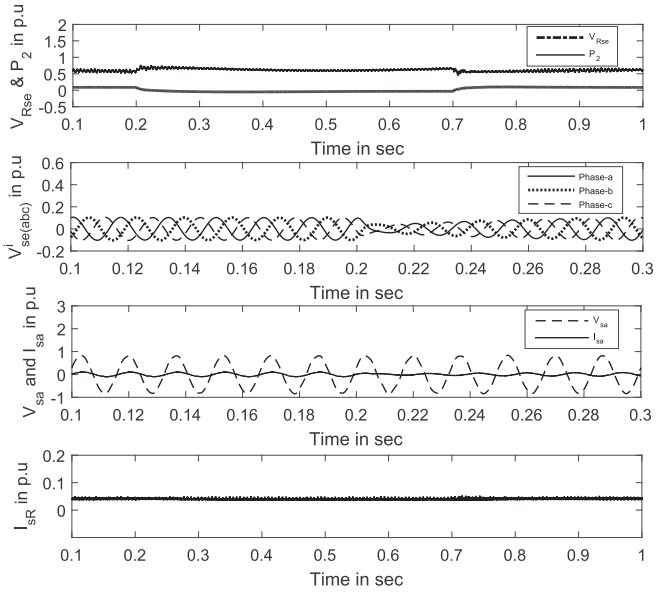


Fig. 14. Step response to the series converter capacitive/inductive mode transition of the series injected reactive voltage ($V_{\mathrm{Rse}}$), active power in the line ($P_2$), series injected three-phase voltages ($V^i_{\mathrm{se(abc)}}$), phase-$a$ of AC bus voltage ($V_{sa}$)/shunt converter current ($I_{sa}$), and the shunt converter reactive current ($I_{sR}$).

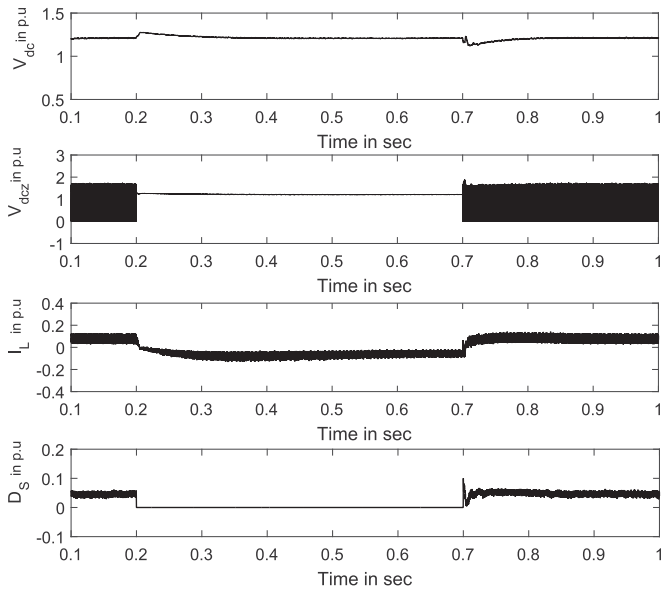


Fig. 15. Step response of the dc-link capacitor voltage ($V_{\mathrm{dc}}$), series converter DC voltage ($V_{\mathrm{dcz}}$), inductor current ($I_L$), and the shoot through duty ratio ($D_S$) to the series converter capacitive/inductive mode transition.

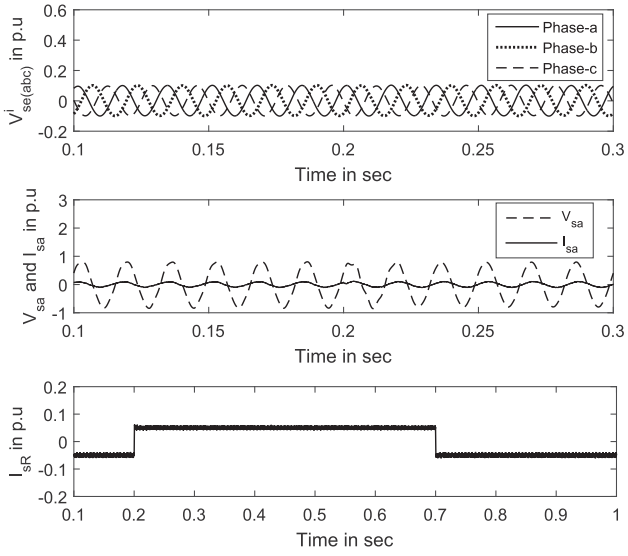


Fig. 16. Step response of series-injected three-phase voltages ($V^i_{\mathrm{se(abc)}}$), phase-a of AC bus voltage ($V_{sa}$)/shunt converter current ($I_{sa}$) and shunt converter reactive current ($I_{sR}$) for shunt converter capacitive/inductive mode transitions.

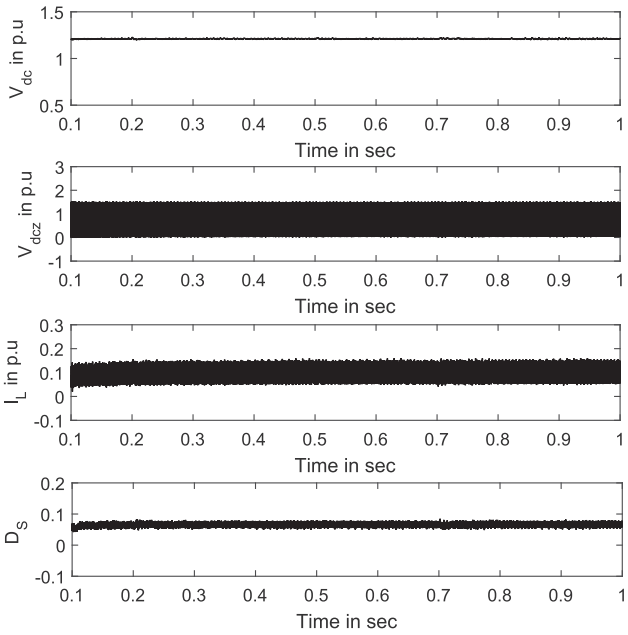


Fig. 17. Step response of dc-link capacitor voltage ($V_{\mathrm{dc}}$), series converter DC voltage ($V_{\mathrm{dcz}}$), inductor current ($I_L$) and shoot-through duty ratio ($D_S$) for shunt converter capacitive/inductive mode transitions.

is applied at 0.2 s, and is removed at 0.7 s. We note from Fig. 16 that as the reactive current changes from capacitive to inductive, and that the phase angle of the shunt converter current changes from leading to lagging. Also from Fig. 17, we observe that there is no significant variation in the dc-link capacitor voltage, and that the performance of other transient responses ($V_{\mathrm{dcz}}$, $I_L$, and $D_S$) are satisfactory.

From the results in Figs. 16 and 17, we conclude that the boost mode of the Z-network can maintain the series converter DC voltage at the specified value despite the dwindling in the dc-link capacitor voltage. As such, the boost function of Z-network supports the series converter in providing the desired series compensation in a long transmission line. As a result, the incorporation of the Z-network (in UPFC) could help to reduce the power rating of the shunt converter and the dc-link capacitor, and hence reduce the overall cost of UPFC.

We observe from Figs. 7, 8, 10, and 11 that the main advantages of the proposed ZSC-UPFC over conventional VSC-UPFC are threefold.

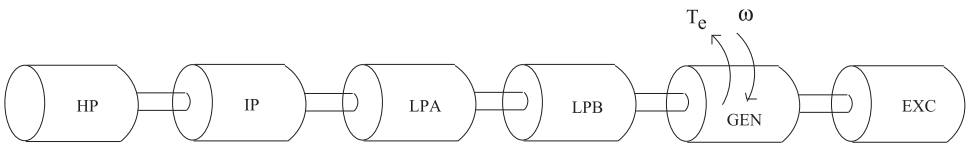


Fig. 18. Six mass mechanical system.

1) At the operating point, ZSC-UPFC can inject comparatively higher series active and reactive voltages than VSC-UPFC of the same capacity;

2) ZSC-UPFC requires smaller size of shunt converter and DC capacitor than VSC-UPFC to control power flow in the same transmission line;

3) under varying operation conditions of the dc-link capacitor, ZSC-based series converter can inject the desired AC voltage with steady DC boosted voltage.

## V. Conclusion

In this paper, we propose a ZSC-UPFC configuration to enhance the power control for long transmission lines. The incorporation of the Z-network in UPFC provides DC voltage boost for the series converter. We carry out transient analysis for the three-phase model of the proposed ZSC-UPFC. In this three-phase model of ZSC-UPFC, the converter operation is modeled by switching functions. We use the SVPWM technique to generate the switching function of converters. The performance of the combined system with the proposed ZSC-UPFC configuration is validated by extensive transient simulation. Our simulation results demonstrate the effectiveness of the proposed ZSC-UPFC.

1) The use of the Z-network between the dc-link capacitor and the series converter provides DC voltage boost for the series converter.
2) The boost function of the Z-network supports the series converter compensation for the long transmission line.
3) The proposed ZSC-UPFC configuration ensures the control of the voltage injected by the series converter even with reduced dc-link voltage setting. Subsequently, the active power drawn from the AC bus reduces.
4) Under varying operation conditions of the dc-link capacitor, ZSC-based series converter can inject the desired AC voltage with steady DC boosted voltage.
5) At different operating modes, the ZSC-UPFC effectively controls both the active and reactive power flows in the long transmission line in addition to AC bus voltage control.
6) The implementation of the Z-network can reduce the power rating of the shunt converter and the dc-link capacitor.

## Appendix

## System Parameters of IEEE FBM With ZSC-UPFC

In this appendix, we present the parameters of the IEEE FBM model with 892.4 MVA, 500 kV base. The base frequency is taken as 60 Hz.

### A. Generator Parameters

The subscript $d$ and $q$ represents quantities associated with the direct and quadrature axis, respectively:

1) reactance $x_d = 1.79$, transient reactance $x_d^{'} = 0.169$, subtransient reactance $x_d^{''} = 0.135$;
2) reactance $x_q = 1.71$, transient reactance $x_q^{'} = 0.228$, subtransient reactance $x_q^{''} = 0.200$;
3) armature resistance $R_a = 0$;
4) open-circuit transient constant $T_{do}^{'} = 4.3$, open-circuit subtransient constant $T_{do}^{''} = 0.032$;
5) open-circuit transient constant $T_{qo}^{'} = 0.85$, open-circuit subtransient constant $T_{qo}^{''} = 0.05$;
6) short-circuit transient constant $T_d^{'} = 0.4000$, short-circuit subtransient constant $T_d^{''} = 0.0259$;
7) short-circuit transient constant $T_q^{'} = 0.1073$, short-circuit subtransient constant $T_q^{''} = 0.0463$.

### B. Multimass Mechanical System

Fig. 18 shows the six mass mechanical system adopted in our simulation. The self-damping for the high pressure (HP), intermediate pressure (IP), low pressure-A (LPA), and low pressure-B (LPB) turbines is set to be 0.20. The mutual dampings between HP-IP, IP-LPA, LPA-LPB, and LPB-GEN are set as 0.30, whereas the mutual damping between generator exciter (GEN-EXC) is 0.005. The fraction of the total torque allocated to HP, IP, LPA, and LPB turbines is 0.30, 0.26, 0.22, and 0.22, respectively.

### C. Transformer and Transmission Line Parameters

$R_t = 0.00$, $X_t = 0.14$, $R_1 = 0.0144$, $X_1 = 0.36$, $R_2 = 0.0176$, $X_2 + X_{sys} = 0.5$.

### D. ZSC-UPFC Parameters

*1) Z-network:* Capacitive susceptance $b_{c1} = b_{c2} = 0.12$, inductive reactance $X_{L1} = X_{L2} = 0.06$, resistance $r = R = 0.001$.

*2) Shoot-through duty ratio controller parameters:* $K_{p(\mathrm{vdcz})} = 1.5$, $K_{i(\mathrm{vdcz})} = 50$, $K_{p(\mathrm{iL})} = 35$. Here, $K_p$ and $K_i$ refer to the proportional and integral gain (for different controllers), respectively.

*3) Shunt VSC:* The rating of shunt VSC is 150 MVA with $R_{\mathrm{sh}} = 0.01$, $X_{\mathrm{sh}} = 0.15$. The dc-link capacitor is with susceptance $b_c = 1.5$ and conductance $g_p = 1/78.7$ (cf. Fig. 1).

*4) Shunt controller parameters:* $K_{p(\mathrm{vdc})} = 0.5$, $K_{i(\mathrm{vdc})} = 10$, $K_{p(\mathrm{ipsh})} = 25$, $K_{i(\mathrm{ipsh})} = 2000$. $K_{p(\mathrm{qs})} = 1.5$, $K_{i(\mathrm{qs})} = 50$, $K_{p(\mathrm{irsh})} = 50$, $K_{i(\mathrm{irsh})} = 4000$.

*5) The rating of the series VSC:* 150 MVA.

*6) Series controller parameters:* $K_{p(\mathrm{xse})} = 0.15$, $K_{i(\mathrm{xse})} = 15$, $K_{p(\mathrm{rse})} = 1.4$, $K_{\mathrm{i(rse)}} = 50$.

## REFERENCES


[1] N. G. Hingorani and L. Gyugyi, *Understanding FACTS*. New York, NY, USA: IEEE Press, 2000.

[2] K. R. Padiyar, *FACTS Controllers in Power Transmission and Distribution*. New Delhi, India: New Age Int., 2007.

[3] M. Rahman, M. Ahmed, R. Gutmna, R. J. O. Keefe, R. Nelson, and J. Bian, "UPFC application on the AEP system: Planning considerations," *IEEE Trans. Power Syst.*, vol. 12, no. 4, pp. 1695–1701, Nov. 1997.

[4] A. Arabi and P. Kundur, "A versatile FACTS device model for power-flow and stability simulations," *IEEE Trans. Power Syst.*, vol. 11, no. 4, pp. 1994–1950, Nov. 1996.

[5] A. Nabavi-Niaki and M. R. Iravani, "Steady state and dynamic model of unified power flow controller (UPFC) for power system studies," *IEEE Trans. Power Syst.*, vol. 11, no. 4, pp. 1937–1934, Nov. 1996.

[6] K. R. Padiyar and N. Prabhu, "Design and performance evaluation of subsynchronous damping controller with STATCOM," *IEEE Trans. Power Del.*, vol. 21, no. 3, pp. 1398–1405, Jul. 2006.

[7] K. R. Padiyar and N. Prabhu, "Investigation of SSR characteristics of unified power flow controller," *Elect. Power Syst. Res.*, vol. 74, pp. 211–221, 2005.

[8] R. Mihilac, P. Zunko, and D. Povh, "Improvement of transient stability using unified power flow controller," *IEEE Trans. Power Del.*, vol. 11, no. 1, pp. 485–491, Jan. 1996.

[9] K. R. Padiyar and K. U. Rao, "Modeling and control of unified power flow controller for transient stability," *Elect. Power Energy Syst.*, vol. 21, no. 1, pp. 1–11, Jan. 1999.

[10] K. K. Sen and E. J. Stacy, "UPFC-unified power flow controller: Theory, modelling and applications," *IEEE Trans. Power Del.*, vol. 13, no. 4, pp. 1453–1460, Oct. 1998.

[11] X. Lombard, and P. G. Themod, "Control of unified power flow controller: Comparison of methods on the basis of a detailed numerical model," *IEEE Trans. Power Syst.*, vo1. 12, no. 2, pp. 824–830, May 1997.

[12] K. Chakravarthy, R. Saleem, and D. Singh, "Power flow improvement in transmission line using UPFC," *IEEE Trans. Power Syst.*, vo1. 9, no. 3, pp. 1454–1461, Jun. 2014.

[13] B. Ge *et al.*, "An energy stored quasi-Z-source inverter for application to photovoltaic power system," *IEEE Trans. Ind. Electron.*, vol. 60, no. 10, pp. 4468–4481, Oct. 2013.

[14] C. J. Gajanayake, D. M. Vilathgamuwa, P. C. Loh, R. Teodorescu, and F. Blaabjerg, "Z-source inverter based flexible distributed generation system solution for grid power quality improvement," *IEEE Trans. Energy Convers.*, vol. 24, no. 3, pp. 695–704, Sep. 2009.

[15] M. Shen, A. Joseph, J. Wang, F. Z. Peng, and D. J. Adams, "Comparison of traditional inverters and Z-source inverter for fuel cell vehicles," *IEEE Trans. Power Electron.*, vol. 22, no. 4, pp. 1453–1463, Jul. 2007.

[16] D. M. Vilathgamuwa, C. J. Gajanayake, P. C. Loh, and Y. W. Li, "Voltage sag compensation with Z-source inverter based dynamic voltage restorer," in *Proc. Conf. Rec. IEEE Ind. Appl. Conf. 41st IAS Annu. Meeting*, Oct. 2006, pp. 2242–2248.

[17] H. Fujita, H. Akagi, and Y. Watanabe, "Dynamic control and performance of a unified power flow controller for stabilizing an AC transmission system," *IEEE Trans. Power Electron.*, vol. 21, no. 4, pp. 1013–1020, Jul. 2006.

[18] K. R. Padiyar and A. M. Kulkarni, "Control design and simulations of unified power flow controller," *IEEE Trans. Power Del.*, vo1. 13, no. 4, pp. 1348–1354, Oct. 1998.

[19] K. Sreenivasachar, "Unified power flow controller: Modeling, stability analysis, control strategy and control system design," Ph.D thesis, Univ. Waterloo, ON, Canada, 2001.

[20] I. Papic, P. Zunko, and D. Povh, "Basic control of unified power flow controller," *IEEE Trans. Power Syst.*, vol. 12, no. 4, pp. 1734–1739, Nov. 1997.

[21] J. Wang and F. Z. Peng, "Unified power flow controller using the cascade multilevel inverter," *IEEE Trans. Power Electron.*, vol. 19, no. 4, pp. 1077–1084, Jul. 2004.

[22] A. K. Sadigh, M. T. Hagh, and M. Sabahi, "Unified power flow controller based on two shunt converters and a series capacitor," *Elect. Power Syst. Res.*, vol. 80, no. 12, pp. 1511–1519, Dec. 2010.

[23] K. R. Padiyar, *Analysis of Subsynchronous Resonance in power systems*. Boston, MA, USA: Kluwer, 1999.

[24] R. Thirumalaivasan, M. Janaki, and N. Prabhu, "Damping of SSR using subsynchronous current suppressor with SSSC," *IEEE Trans. Power Syst.*, vol. 28, no. 1, pp. 64–74, Feb. 2013.

[25] F. Z. Peng, "Z-source inverter," *IEEE Trans. Ind. Appl.*, vol. 39, no. 2, pp. 504–510, Mar. 2003.

[26] J. Liu, J. Hu, and L. Xu, "Dynamic modeling and analysis of Z source converter derivation of AC small signal model and design-oriented analysis," *IEEE Trans. Power Electron.*, vol. 22, no. 5, pp. 1786–1796, Sep. 2007.

[27] P. C. Loh, D. M. Vilathgamuwa, C. J. Gajanayake, Y. R. Lim, and C. W. Teo, "Transient modeling and analysis of pulse-width modulated Z-source inverter," *IEEE Trans. Power Electron.*, vol. 22, no. 2, pp. 498–507, Mar. 2007.

[28] S. Rajakaruna and L. Jayawickrama, "Steady-state analysis and designing impedance network of Z-source inverters," *IEEE Trans. Ind. Electron.*, vol. 57, no. 7, pp. 2483–2491, Jul. 2010.

[29] Y. P. Siwakoti, F. Z. Peng, F. Blaabjerg, P. C. Loh, and G. E. Town, "Impedance-source networks for electric power conversion part I: A topological review," *IEEE Trans. Power Electron.*, vol. 30, no. 2, pp. 699–716, Feb. 2015.

[30] Y. P. Siwakoti, F. Z. Peng, F. Blaabjerg, P. C. Loh, G. E. Town, and S. Yang, "Impedance-source networks for electric power conversion Part II: Review of control and modulation techniques," *IEEE Trans. Power Electron.*, vol. 30, no. 4, pp. 1887–1906, Apr. 2015.

[31] H. Abu-Rub, M. Malinowski, and K. Al-Haddad, *Power Electronics for Renewable Energy Systems, Transportation and Industrial Applications*. Chichester, U.K.: IEEE Press—Wiley, 2014.

[32] F. B. Effah, P. Wheeler, J. Clare, and A. Watson, "Space-vector-modulated three-level inverters with a single Z-source network," *IEEE Trans. Power Electron.*, vol. 28, no. 6, pp. 2806–2815, Jun. 2013.

[33] Y. Kun, "Space vector pulse-width modulation theory and topology improvement for Z-source inverters," Ph.D. thesis, Nanyang Technol. Univ., Singapore, 2012.

[34] "First bench mark model for computer simulation of subsynchronous resonance," *IEEE Trans. Power App. Syst.*, vol. PAS-96, no. 5, pp. 1565–1572, Sep. 1977.

[35] L. Xu, L. Yao, and C. Sasse, "Grid integration of large DFIG-based wind farms using VSC transmission," *IEEE Trans. Power Electron.*, vol. 22, no. 3, pp. 976–984, Aug. 2007.

[36] *Using MATLAB-SIMULINK*, MathWorks, Inc., Natick, MA, USA, 1999.


**R. Thirumalaivasan** (M'12) received the B.E. degree in electrical and electronics engineering from Madras University, Chennai, India, in 1999, the M.Tech. degree in laser and electrooptical engineering from Anna University, Chennai, India, in 2002, and the Ph.D. degree from the Department of Electrical Engineering, Jawaharlal Nehru Technological University, Hyderabad, India, in 2014.

He is an Associate Professor in the School of Electrical Engineering, VIT University, Vellore, India, and currently working as a Postdoctoral Researcher in the Engineering Systems Design pillar at SUTD, Singapore. His research interests include FACTS, HVDC, and real-time digital simulation of power electronics and power systems.

**Yunjian Xu** (S'06–M'10) received the B.S. and M.S. degrees in electrical engineering from Tsinghua University, Beijing, China, in 2006 and 2008, respectively, and the Ph.D. degree in communications and networks from the Massachusetts Institute of Technology (MIT), Cambridge, MA, USA, in 2012.

He was a CMI (Center for the Mathematics of Information) Postdoctoral Fellow at the California Institute of Technology, Pasadena, CA, USA, in 2012–2013. Before he joined the Chinese University of Hong Kong as an assistant professor in 2017, he was an assistant professor at the Singapore University of Technology and Design in 2013–2017. His research interests include energy systems and markets, with emphasis on power system control and optimization, wholesale electricity marketdesign, and the aggregation of distributed energy resources in power distribution systems. He received the MIT-Shell Energy Fellowship.

**M. Janaki** (M'12) received the B.E. degree in electrical and electronics engineering from Madras University, Chennai, India, in 1996, M.E. degree in control and instrumentation from Anna University, Chennai, India, in 2002, and the Ph.D. degree from the Department of Electrical Engineering, Jawaharlal Nehru Technological University, Hyderabad, India, in 2015.

She is an Associate Professor in the School of Electrical Engineering, VIT University, Vellore, India. Her research interests include FACTS, HVDC, and power systems.